

Lost in Backpropagation: The LM Head is a Gradient Bottleneck

Nathan Godey¹ Yoav Artzi¹

Abstract

The last layer of neural language models (LMs) projects output features of dimension D to logits in dimension V , the size of the vocabulary, where usually $D \ll V$. This mismatch is known to raise risks of limited expressivity in neural LMs, creating a so-called softmax bottleneck. We show the softmax bottleneck is not only an expressivity bottleneck but also an optimization bottleneck. Backpropagating V -dimensional gradients through a rank- D linear layer induces unavoidable compression, which alters the training feedback provided to the vast majority of the parameters. We present a theoretical analysis of this phenomenon and measure empirically that 95-99% of the gradient norm is suppressed by the output layer, resulting in vastly suboptimal update directions. We conduct controlled pretraining experiments showing that the gradient bottleneck makes trivial patterns unlearnable, and drastically affects the training dynamics of LLMs. We argue that this inherent flaw contributes to training inefficiencies at scale independently of the model architecture, and raises the need for new LM head designs.

1. Introduction

There is significant research effort focusing on developing new architectures for the hidden layers of language models (LMs), aiming to improve efficiency and performance at training and inference times (e.g. Gu & Dao, 2024; Ye et al., 2025; Yang et al., 2025). Despite fundamental differences, all considered architectures share a common structure for the output layer: a single linear mapping, followed by a softmax. This component is often called the *LM head*. In other words, most autoregressive LMs can be seen as (potentially massive) feature extractors for a multi-class classifier, where classes correspond to tokens.

The LM head design is a standard choice for multi-class classification. However, the language modeling classifica-

¹Cornell University, New York. Correspondence to: Nathan Godey <godeynathan@gmail.com>.

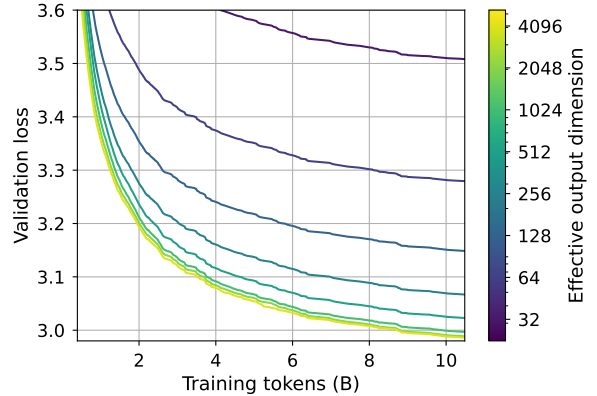


Figure 1. Training dynamics for 2B models with different dimensionality constraints on the LM head. We control the rank of the output linear layer to mimic reduced hidden dimensions without changing the shape of the Transformers backbone. The results illustrate how the softmax bottleneck alone significantly reduces the convergence speed. More details can be found in Section 3.1.

tion setup itself is fairly unusual: the number of extracted features, i.e. the hidden dimension D of the model, is commonly orders of magnitude smaller than the number of classes, i.e. the token vocabulary size V . This mismatch has been shown to limit the expressivity of LMs, and may lead to representation degeneration and performance saturation for small models (Yang et al., 2018; Ganea et al., 2019; Godey et al., 2024). Yet, an important aspect of this mismatched mechanism has so far been ignored: *the loss gradients in the high-dimensional logit space are backpropagated to a lower-dimension space* before the backward pass reaches the rest of the layers. In this work, we frame the softmax bottleneck not as an expressivity issue but instead as a significant factor in training dynamics, where stronger bottlenecks hurt the data efficiency of LMs regardless of the underlying architectural choices.

We show both empirically and theoretically that the softmax bottleneck induces lossy compression during backpropagation, destroying $>95\%$ of the gradient norm. Low-rank LM heads hamper optimization dynamics, making some trivial patterns unlearnable (Section 3.2), and reducing LLM training efficiency by up to $\times 16$ for the same backbone (Section 3.1). Our work sheds light on a so far overlooked weakness in current LLM design, outlining important direc-

tions for future work.¹

Our main contributions are:

- A theoretical analysis of the gradient bottleneck at the LM head, analyzing the structure of the logit gradient under mild assumptions, showing that part of the gradient is inevitably suppressed during backpropagation;
- A set of 2B parameter LMs with varying controlled bottlenecks, showing that training convergence speed is increasingly affected as the bottleneck gets stronger, with noticeable gaps up to our maximum tested hidden dimension (4,096);
- An example of a trivial synthetic language where expressivity is not an issue, but for which the gradient bottleneck makes it increasingly harder for the model to learn correctly;
- Empirical demonstration that the gradient bottleneck destroys 95-99% of the gradient norm, and that it transfers energy from the most important part of the backpropagation signal to the tail of the coefficients in the form of random noise.

2. Theoretical Analysis

2.1. Setup: Notation and Loss Formulation

We express the language modeling objective in a matrix form that will allow us to analyze both expressivity and gradient flow through the LM head.

We model language as a probability distribution P over token sequences $(w_t)_{t=1}^L$, where tokens take values in a vocabulary of size V . We observe a dataset

$$X = (w_{s,t})_{s=1,\dots,S; t=1,\dots,L_s}$$

sampled from P , with S the number of sampled sequences and L_s the length of sequence $s \in [1, S]$. The standard maximum likelihood objective for a language model $(\varphi_\theta, W_\theta)$ can then be written as:

$$\mathcal{L}(\theta, X) = -\frac{1}{T} \sum_{s,t} \langle \mathbf{1}_{w_{s,t}}, \log \sigma(W_\theta \varphi_\theta(\mathbf{w}_{s,<t})) \rangle, \quad (1)$$

where $T = \sum_s L_s$, $W_\theta \in \mathbb{R}^{V \times D}$, φ_θ maps contexts to \mathbb{R}^D , and σ denotes the softmax. Intuitively, in Transformers, $W_\theta \in \mathbb{R}^{V \times D}$ is the LM head projection and φ_θ is the rest of the network (i.e. below the LM head). The log function is taken element-wise, and we extend it as $\log 0 = 0$ for the sake of simplicity.²

Fully Expressive Representations We assume that φ_θ is deterministic and sufficiently expressive so that each

distinct context $c = \mathbf{w}_{s,<t}$ can be assigned any vector $\varphi_\theta(c) = h_c \in \mathbb{R}^D$ without loss of generality. Under this assumption, optimization over θ is equivalent to optimization over parameters $\{h_c\}$ and W .

We rewrite the conventional log-likelihood loss in matrix notation, similar to Yang et al. (2018). Let \mathcal{C} be the set of distinct contexts observed in X , with $|\mathcal{C}| = C$, and the next-token count vector for context $c \in \mathcal{C}$ be:

$$N_c = \sum_{s,t} \delta_{c=\mathbf{w}_{s,<t}} \mathbf{1}_{w_{s,t}} \in \mathbb{N}^V. \quad (2)$$

Stacking these into a matrix $N \in \mathbb{R}^{C \times V}$ and letting $H \in \mathbb{R}^{C \times D}$ denote the matrix of context representations (i.e. the representation before the LM head), the loss can be written compactly as:

$$\mathcal{L} = -\frac{1}{T} \langle N, \log \sigma(HW^\top) \rangle_F. \quad (3)$$

2.2. Expressivity and the Softmax Bottleneck

The classical expressivity view of the softmax bottleneck is that the LM head imposes a rank constraint on the model’s output log-probabilities, which can prevent the model from matching the true data distribution. We show, however, that this rank constraint does not affect top-1 predictions, motivating a closer look at the *optimization* consequences in Section 2.3.

First, we revisit the characterization of the optimal achievable likelihood under no rank constraints.

Proposition 2.1 (Gibbs inequality). *Let \tilde{N} denote the row-normalized version of N . Then*

$$\mathcal{L} \geq -\frac{1}{T} \langle N, \log \tilde{N} \rangle_F, \quad (4)$$

with equality if and only if $\sigma(HW^\top) = \tilde{N}$.

This proposition identifies the empirical conditional distributions \tilde{N} as the unconstrained optimum. However, the equality condition is typically unattainable due to rank constraints on HW^\top .

Proposition 2.2 (Yang et al. 2018). *We have*

$$\text{rank}(HW^\top) \leq D, \quad \text{rank}(\log \sigma(HW^\top)) \leq D + 1.$$

Proof. The first inequality is immediate. For the second, observe that for any matrix A , each row of $\log \sigma(A)$ equals $A_i - z_i \mathbf{1}$, where z_i is the log of the softmax denominator. This implies that the row space is spanned by that of A together with the all-ones vector, and thus has a rank bounded by $\text{rank}(A) + 1$. \square

¹Code, data and checkpoints will be released shortly.

²See Appendix B for a discussion on this choice.

Corollary 2.3 (Yang et al. 2018). *We assume $\forall i, j, \tilde{N}_{ij} > 0$. The empirical minimum for Equation (3) is attainable if and only if*

$$\text{rank}(\log \tilde{N}) \leq D + 1 .$$

This result formalizes the softmax bottleneck: even with perfect context representations, the output layer imposes a strict low-rank constraint on realizable log-probabilities. In other words, when $D \ll V$, the model simply cannot assign arbitrary probability distributions over the vocabulary, regardless of how the backbone is trained.

However, this expressivity limitation does not prevent the model from correctly identifying the *most likely* next token and its probability up to arbitrary precision when $D \geq 2$:

Proposition 2.4 (Proof in Appendix A.1). *When $D \geq 2$, for all $\varepsilon > 0$ and $i \in [1, C]$, there exists H, W so that:*

$$\left| \sigma(H_i W^\top)_{i, \arg \max(\tilde{N}_i)} - \tilde{N}_{i, \arg \max(\tilde{N}_i)} \right| < \varepsilon . \quad (5)$$

Therefore, even though the low-rank constraint limits the model expressivity, the set of reachable top-1 probabilities is not constrained, and the overall behavior of the language model is theoretically unaffected for greedy decoding. This means that the softmax bottleneck cannot be fully characterized as an expressivity issue alone, and motivates us to examine it through the lens of optimization dynamics.

2.3. The Gradient Descent Viewpoint

Our analysis shows how the softmax bottleneck affects *training*, not just expressivity. The key insight is that backpropagating through the LM head compresses the gradient from V dimensions down to at most D dimensions, discarding the majority of the training signal. We formalize this by tracking how the logits evolve under gradient descent, and showing that the resulting update direction is fundamentally misaligned with the logit gradient whenever $D \ll V$.

Recall that the logits (i.e. the activations after the LM head projection, but before the softmax) are given by

$$L_\theta^\tau = H_\theta^\tau (W_\theta^\tau)^\top ,$$

where τ denotes the gradient descent iteration. Understanding how L_θ^τ evolves is crucial, because the loss depends on θ only through the induced probability matrix $P_\theta^\tau = \sigma(L_\theta^\tau)$.

Logit Dynamics Under Gradient Descent Let $P_\theta^\tau = \sigma(L_\theta^\tau)$, and define the empirical context weights

$$\omega_i = \frac{\sum_j N_{ij}}{T} .$$

The LM head update with learning rate η is given by

$$W_\theta^{\tau+1} = W_\theta^\tau - \eta \cdot (P_\theta^\tau - \tilde{N})^\top \text{diag}(\omega) H_\theta^\tau .$$

Effective update direction. For convenience, we define the rescaled logit update

$$\Delta_\theta^\tau = \frac{L_\theta^{\tau+1} - L_\theta^\tau}{\eta} .$$

By construction, Δ_θ^τ is a sum of two matrices whose ranks are upper-bounded by D , which implies that

$$\text{rank}(\Delta_\theta^\tau) \leq 2D . \quad (6)$$

As a consequence, however large V may be, the actual global logit update is at most rank $2D$. By contrast, if the logits were optimized directly, i.e. if we performed gradient descent on the logit matrix taken as a parameter, the first-order optimal update direction in the limit $\eta \rightarrow 0$ would be given by the logit gradient

$$\nabla_L \mathcal{L}(\theta^\tau, X) = \text{diag}(\omega)(P_\theta^\tau - \tilde{N}) . \quad (7)$$

The central question is therefore: *under which conditions can the actual update direction Δ_θ^τ induced by gradient descent (Equation (6)) match the logit-optimal direction (Equation (7))?* Answering this question requires analyzing the structure and rank properties of $(P_\theta^\tau - \tilde{N})$.

Rank of the Prediction Error We begin by identifying contexts for which the empirical next-token distribution is degenerate.

Proposition 2.5 (Proof in Appendix A.2). *Consider the set of contexts*

$$C^u = \{\mathbf{w}_{s, < t} \mid \tilde{N}_{w_{s,t}} = \delta_{w_{s,t}}\}$$

for which the empirical next-token probability is concentrated on a single token. Let

$$C^{uu} = \{w_{s,t} \mid \mathbf{w}_{s, < t} \in C^u\}$$

denote the set of corresponding unique next tokens. If $P \in (0, 1)^{C \times V}$, then

$$\text{rank}(P - \tilde{N}) \geq \min(|C^{uu}|, V - 1) := \mathcal{D}^u(N) .$$

Informally, this says that as long as many distinct tokens each appear as the unique observed continuation of some context, the prediction error matrix $(P - \tilde{N})$ has very high rank, close to V .

In natural language, it is reasonable to expect that most tokens appear at least once in a context where the observed continuation is unique in the training set, especially for long sequences. Some continuations are even constrained by the language distribution, e.g., *earth* following *down-to-*. This motivates the hypothesis that in practical language modeling setups $|C^{uu}| \simeq V$, or at least $|C^{uu}| \gg D$. We corroborate these arguments with experimental observations in Appendix C.

Mismatch Between Ideal and Realizable Updates Combining the rank lower bound on $(P - \tilde{N})$ from [Proposition 2.5](#) with the rank upper bound on Δ_θ^τ from [Equation \(6\)](#), we can now quantify the inevitable gap between the actual update and the logit gradient.

Proposition 2.6 (Update direction residual). *If $\mathcal{D}^u(N) > D$, then*

$$\|\Delta_\theta^\tau - (P_\theta^\tau - \tilde{N})\|_F > \sqrt{\sum_{i=2D+1}^{\mathcal{D}^u(N)} \zeta_i^2} > 0 ,$$

where ζ_i are the singular values of $(P_\theta^\tau - \tilde{N})$ in decreasing order.

Proof. This is a direct application of the Eckart–Young–Mirsky theorem. \square

In other words, whenever the logit gradient has intrinsic rank exceeding $2D$, which [Proposition 2.5](#) shows to be the typical case, no gradient descent step through a rank- D LM head can match it. The missing components correspond to the tail singular values of $(P - \tilde{N})$, and the bound worsens as D decreases. In that sense, the LM head is a gradient bottleneck.

2.3.1. STOCHASTIC GRADIENT DESCENT

One might hope that stochastic gradient descent (SGD) mitigates this issue: mini-batches see only a subset of contexts, so the effective $\tilde{N}^\mathcal{B}$ within a batch could in principle have lower rank, relaxing the bottleneck. This is not the case though. The high-rank structure of the logit gradient persists in the SGD setting, particularly as the model approaches convergence.

Notation. Consider a batch $\mathcal{B} \in \mathcal{P}([1, S])$, where S is the number of sequences in our observed dataset X . This batch contains contexts $\mathcal{C}_\mathcal{B} \in \mathcal{P}(\mathcal{C})$. Let $N^\mathcal{B}$ and $\tilde{N}^\mathcal{B}$ be the in-batch context-token count matrix and its row-normalized version, and $(P_\theta^\tau)_\mathcal{B}$ the matrix extracted from P_θ^τ by retaining rows corresponding to contexts in $\mathcal{C}_\mathcal{B}$.

Proposition 2.7 (Proof in [Appendix A.3](#)). *Let $\mathcal{C}_\mathcal{B}^u$ be the set of contexts c that:*

- have a unique and distinct next token w_c in the batch \mathcal{B} while having several observed next tokens in the dataset X ;
- are such that $(\tilde{N}_{cw_c'})_{c,c' \in \mathcal{C}_\mathcal{B}^u}$ is analogous to the adjacency matrix of a connected graph.

There exists $\varepsilon_\mathcal{B} > 0$ such that if

$$\max_{c \in \mathcal{C}_\mathcal{B}^u} \|(P_\theta^\tau)_c - \tilde{N}_c\|_\infty < \varepsilon_\mathcal{B} \quad (8)$$

then

$$\text{rank}((P_\theta^\tau)_\mathcal{B} - \tilde{N}^\mathcal{B}) \geq \mathcal{D}^\mathcal{B}(N) := \min(|\mathcal{C}_\mathcal{B}^u|, V - 1) .$$

[Proposition 2.7](#) indicates that when the model predictions P_θ^τ get closer to the empirical data distribution \tilde{N} , the first-order optimal logit update direction for batch \mathcal{B} is high-rank and the actual logits update is therefore suboptimal, by the same mechanism as in [Proposition 2.6](#).

Corollary 2.8. *We assume that θ is such that*

$$\forall \mathcal{B}, |\mathcal{C}_\mathcal{B}^u| \geq V - 1 .$$

Then, we have:

$$\|\Delta_{\mathcal{B}\theta}^\tau - ((P_\theta^\tau)_\mathcal{B} - \tilde{N}^\mathcal{B})\|_F > \sqrt{\sum_{i=2D+1}^{V-1} \zeta_i^2} > 0 ,$$

where ζ_i are the singular values of $(P_\theta^\tau)_\mathcal{B} - \tilde{N}^\mathcal{B}$ in decreasing order.

Taken together, [Proposition 2.7](#) and [Proposition 2.8](#) show that the gradient bottleneck is not an artifact of full-batch training: near convergence, even mini-batch gradients are high-rank, and the rank- D LM head remains a fundamental obstacle.

The weakness of the connectivity condition in [Proposition 2.7](#) is justified for natural language because special and frequent tokens should often have non-null probability and thus behave similarly to high-degree vertices. Many next-token probability distributions should also have relatively high entropy and increase connectivity. We provide empirical elements to back these arguments in [Appendix C](#). In practice, for batches containing $10^5 - 10^7$ tokens, the number of positive-entropy contexts that appear only once should not be greatly inferior to V .

Alternative LM Heads One might also wonder whether replacing the standard softmax with a more expressive output layer, as proposed in past work to address the expressivity bottleneck, resolves the optimization issue as well. We show that it does not. Past work ([Yang et al., 2018; 2019; Ganea et al., 2019](#)) has proposed alternatives to the softmax layer to improve the expressivity of models in terms of output probabilities. These alternatives break down the LM head into several components before recombining outputs, which theoretically boosts the maximum rank of the output log-probabilities. However, the proposed alternatives theoretically fail to address the softmax bottleneck from the optimization perspective. Indeed, if we consider any $f_\theta(H_\theta) = L_\theta$, then

$$\nabla_H \mathcal{L}(\theta^\tau, X) = \text{diag}(\omega)(P_\theta^\tau - \tilde{N})J_f(H_\theta) , \quad (9)$$

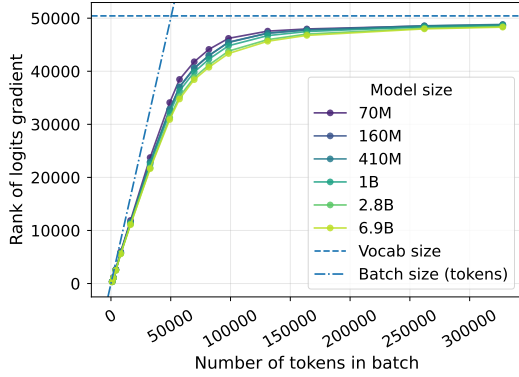


Figure 2. Empirical rank of the logits gradients as the number of batch tokens increases. The dotted blue lines delimit the highest possible rank.

where the Jacobian $J_f(H_\theta)$ is rank D at most. The optimization process is thus limited – in the first-order – by the same effect we described in the softmax case, regardless of the specific form of f .

Nevertheless, even though H_θ never benefits from a complete view of the loss gradient in the logits, some functions f may provide less lossy compression through J_f , potentially through pre-conditioning or regularization. Such alternatives would not target full expressivity, but rather aim to preserve gradient flow through LM heads. We leave the exploration of such methods for future work.

Empirical Validation of the Theory The theoretical results above hint to the fact that logit gradients are near full-rank in practice. We verify this directly: we estimate the empirical ranks of the logits’ gradients of the Pythia models (Biderman et al., 2023) in Figure 2, by measuring them on data taken from the Pile (Gao et al., 2020). We obtain their empirical ranks by counting non-null ($> 1e-6$) diagonal R values in their QR decomposition. It would be insightful to compute singular value distributions for language model heads to estimate the bound given by Proposition 2.8. However, the matrices involved for usual batch sizes (1–4M tokens) are expensive to even store, and computing the SVD of the gradients for 100,000 samples already saturates GPU memory.

3. Experiments

3.1. Consequences on LLM Training

We measure the impact of the gradient bottleneck effect for actual pretraining setups. A difficulty that arises in such experiments is the inherent dependency of model size in the hidden dimension. As a result, studying models with different D values either implies comparing models of different sizes, or adjusting the depth of the models to account

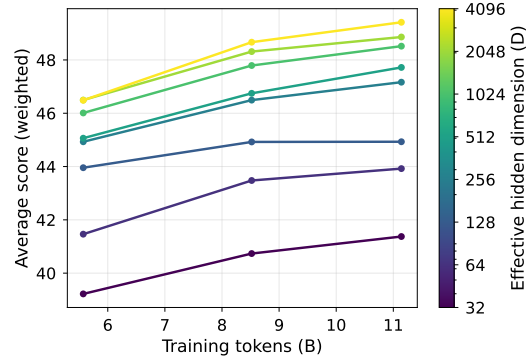


Figure 3. Average zero-shot scores on a subset of downstream tasks for 2B architectures stacked with D -rank LM heads. Average is weighted by benchmark sample size to mitigate variance.

for the increased width. However, prior work (Petty et al., 2024) reports that deeper models show stronger language modeling and downstream performance, which may be a confounding factor in our study.

To disentangle the impact of architectural choices and of the gradient bottleneck effect on performance, we train LMs that share the same Transformer stack, based on the Llama3 architecture, with a hidden dimension of $d_m = 4096$ and 6 hidden layers, representing a total of 1.8B parameters (without the output embeddings). However, the language modeling head of each model mimics a hidden dimension $D \leq d_m$ by adopting a low-rank structure $W_\theta = A_\theta B_\theta$, where $A_\theta \in \mathbb{R}^{V \times D}$ and $B_\theta \in \mathbb{R}^{D \times d_m}$. As a result, the Transformer backbone is equally expressive across all compared models, but D provides control over the strength of the gradient bottleneck.

We train 8 such 2B parameter models on ~ 11 B tokens of Fineweb-Edu data (Penedo et al., 2024), with $D = 2^i$ for $i \in [5, 12]$. To avoid exacerbating the effects of the gradient bottleneck by choosing a large vocabulary, we use the relatively compact SmolLM2 tokenizer (Allal et al., 2025) that counts $V = 49,152$ tokens. We use the WSD learning rate schedule (Hu et al., 2024) to perform cooldown at different points in training (5B, 8.5B, 11B). All details about the pretraining setup can be found in Appendix G. Figure 1 shows the validation loss evolution along training. We perform zero-shot downstream evaluation on our models after LR cooldown in Figure 3. It clearly appears that both the language modeling and downstream performance converge faster for larger values of D . The validation loss of all models is separated by consistent and non-negligible gaps along training. The $D = 4096$ reaches the final loss level of the $D = 32$ variant within 700M tokens, displaying a $\times 16$ speedup in convergence. The final average score gap for $D = 2048$ and $D = 4096$ is $+0.55$, showing a noticeable performance gap even for large hidden dimension. We report detailed scores in Appendix F.

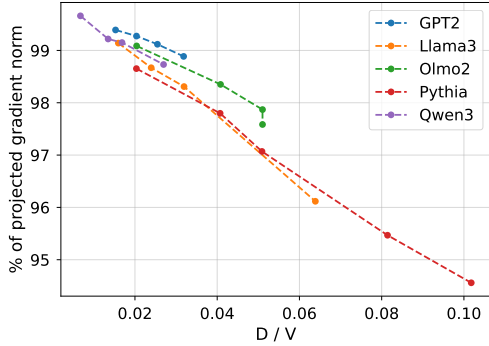


Figure 6. Fraction of the logit gradient norm destroyed by backpropagation as a function of D/V , for several model families.

the null space of W_θ^\top (or more generally $J_f(H_\theta)$), as:

$$\nabla_H \mathcal{L} = \nabla_L \mathcal{L} \cdot J_f(H_\theta)^\top = \nabla_L \mathcal{L} \cdot W_\theta .$$

Hence, the projection of the logits gradient on $\ker(W_\theta^\top)$ is exactly the part of the logits gradient that is destroyed by the gradient bottleneck. We extract a basis for $\ker(W_\theta^\top)$ for different pretrained models by performing a QR decomposition of W_θ and by selecting the trailing $V - D$ columns of Q . We can measure the fraction of the logits gradient norm that is lost in the backpropagation process:

$$\frac{\|p_{\ker(W_\theta)}(\nabla_L \mathcal{L})\|_F}{\|\nabla_L \mathcal{L}\|_F} . \quad (10)$$

Figure 6 reports the fraction of the gradient norm that is destroyed as measured by Equation (10) for several model families: GPT2 (Radford et al., 2019), Pythia (Biderman et al., 2023), Llama3 (AI@Meta, 2024), and Qwen3-Base (Team, 2025). We use 10,000 shuffled documents from the FineWeb dataset (Penedo et al., 2024) as a proxy for usual web-crawled pretraining datasets. We observe that the gradients are almost completely suppressed for all model families, with ~ 95 - 99% of their norm being projected to $\ker(W_\theta^\top)$. We also measure the cosine similarities between projected and original gradients in Appendix D, showing that they are only mildly aligned (0.1-0.2 cosine-similarity). All families follow a similar trend where the fraction of lost logit gradient norm diminishes as D increases.

Figure 7 directly compares the distributions of the coefficients of the full and projected logits gradients for Llama-3.1-70B. The negative coefficient corresponding to the observed token maintains its sign during the projection. The pattern for the first 5 to 10 coefficients is strongly diminished but still correlated with the full gradient. However, the fraction of the norm dedicated to the tail of the coefficients – corresponding to tokens that were predicted with low probability – is more important for the projected gradient. It takes the form of a higher variance, which can be viewed as a form of noise on the training feedback. We perform

the same analysis for Llama-3.1-8B and OLMo2-32B in Appendix E and reach similar conclusions.

3.4. Efficiency of the Update Direction

The training feedback suffers from a destructive compression at the output layer level, which implies a loss of information during the backpropagation process. As a result, the hidden states H_θ and the subsequent model weights are updated based on partial views of the training batch. This raises the question of the efficiency of optimization methods in that setup: to what extent does descending in that compressed direction yield a decrease of the loss on the current training batch?

We answer this question by comparing the loss dynamics for two update directions for the logits: the first-order optimal logits gradient $\nabla_L \mathcal{L}$, and the direction in logit space resulting from updating the hidden states along their gradient, i.e. $\nabla_H \mathcal{L} \cdot W_\theta^\top$. In Figure 8, we extract both directions for several trained models on batches of 1,024 tokens of Fineweb data and compute the loss variation resulting from updating the logits by a fraction of their norm in each direction.

For each family, Figure 8 clearly shows that updating hidden states along $\nabla_H \mathcal{L}$ is orders of magnitude less efficient than directly updating logits along $\nabla_L \mathcal{L}$, given the same budget for the logit update norm. Moreover, updating H along $\nabla_L \mathcal{L}$ is more efficient as the hidden dimension increases, proving that the gradient compression becomes less harmful for update efficiency. This phenomenon is independent of model size, as the loss curves for the 1B and 1.4B Pythia models that share the same hidden dimension hyperparameter collapse into each other. This shows that the gradient compression at the output layer of LLMs is destructive and redirects supervision feedback energy from top components to the tail of the gradient coefficients in the form of noise. This compression harms optimization because the resulting compressed gradients turn out to provide much less efficient update directions for the training loss.

4. Related Works & Discussion

Softmax Bottleneck and Alternatives Yang et al. (2018) are the first to show that softmax-based LMs face an expressivity limitation when the hidden dimension is smaller than the rank of the target log-probability matrix. Chang & McCallum (2022) extended this analysis, showing that a single hidden state cannot simultaneously be close to all possible next-word embeddings, making models unable to represent multi-mode word distributions. Grivas et al. (2022) show that some permutations of next-token probability ordering cannot be reached when $D < V$, but observe rare occurrences of such issues in LMs. To address these expressivity limitations, several architectural alternatives have been pro-

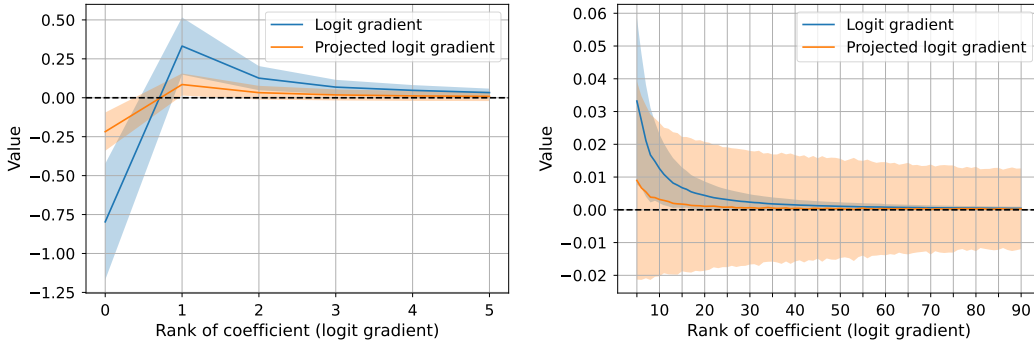


Figure 7. Average full and projected logits gradient coefficients, sorted by absolute values of the full gradient. The gradients are taken for Llama-3.1-70B on Fineweb documents. The plot on the left-hand side focuses on the main coefficients, while the plot on the right-hand side zooms in on smaller coefficients. The standard deviation is reported using filled areas around the curves.

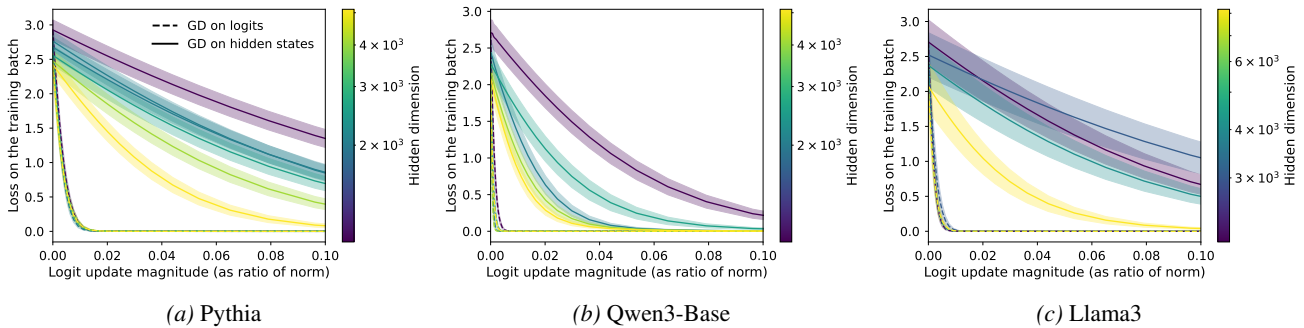


Figure 8. Effect of first-order updates on logits and hidden states for the language modeling loss for different family of models.

posed (Yang et al., 2018; Kanai et al., 2018; Ganea et al., 2019), which all consist in breaking the softmax function into several components to increase the logit rank. While these works focus on the expressivity consequences of the softmax bottleneck, our work reveals a complementary optimization perspective, harming training efficiency and potentially impeding convergence towards expressive weight configurations.

Representation Degeneration and Gradient Flow Gao et al. (2019) identified the representation degeneration problem in neural language generation, observing that output embeddings tend to concentrate in a narrow high-dimensional cone when trained on large datasets. Godey et al. (2024) link this issue to the softmax bottleneck, showing that the emergence of such degeneration can coincide with a performance drop for small LMs. They hypothesize that the softmax bottleneck can lead to optimization issues through unstable dynamics when the LM head reaches a form of spectral saturation. It is unclear whether our findings could shed light on these optimization dynamics, but we argue that even when the representations do not degenerate, the gradient bottleneck effect is still limiting the amount of information that can be backpropagated to the model.

Logit Gradient & Equilibrium Analysis Mircea et al.

(2024) study the loss saturation of Pythia models through an analysis of the logits gradients and exposes a form of tug-of-war effect between positive and negative components that harms learning. Although we do not decompose the logits gradient similarly, we hypothesize that some connections should be made by considering the conservation of sign patterns under the low-rank gradient bottleneck. Finlayson et al. (2024) expose how some patterns of next-token probability emerge through necessary token entanglement in the backpropagation process. While their framing of the softmax bottleneck issue is connected to ours, they only consider implications for expressivity at convergence, and they do not analyze the logits gradients dimensionality in depth.

Discussion & Implications Our findings show that neural LMs suffer from severe gradient compression at their output layer, which represents an inherent limitation for the training efficiency of LLMs. We hypothesize that taking hidden dimensions into account when computing scaling laws (Hoffmann et al., 2022) could help refine their extrapolation quality. A more optimistic view of our work could also indicate that LMs have stronger potential than currently believed, and that convergence speed and/or performance gains could be obtained by better channeling the supervision signal through a better-suited logits prediction module.

Finally, while our work focuses on characterizing the problem, it opens promising directions for innovations that better preserve gradient flow, whether through pre-conditioning, optimization techniques, or well-suited softmax alternatives. These venues may offer substantial gains in training efficiency.

5. Conclusion

We have demonstrated that the softmax bottleneck in neural language models is not merely an expressivity limitation but a fundamental optimization bottleneck. Our theory-grounded empirical analysis shows that 95–99% of the supervision signal is lost during backpropagation through the output layer, in a transfer from informative components to the tail as random noise. Through controlled experiments, we showed that this gradient compression can make even trivial patterns difficult to learn as vocabulary size grows, and significantly slows convergence in realistic 2B parameter pretraining runs. These findings suggest that current LMs train less efficiently than they could. We hope this work inspires renewed attention to this overlooked but critical component of language model architecture.

Acknowledgements

We thank Ryan Cotterell, Andrea Lodi and Jiacheng Liu for useful discussions and insightful feedback in the early stages of this work. We thank the members of the Cornell LIL Lab for their helpful comments, and more specifically Anne Wu for thoughtful suggestions on the manuscript.

This work is partially supported by the National Science Foundation NSF under award OAC-2311521 and NASA under award No. 20-OSTFL20-0053. NG is supported by an Empire AI Postdoctoral Fellowship. We gratefully acknowledge use of the research computing resources of the Empire AI Consortium, Inc, with support from the State of New York, the Simons Foundation, and the Secunda Family Foundation (Bloom et al., 2025).

References

- AI@Meta. Llama 3 model card. 2024. URL https://github.com/meta-llama/llama3/blob/main/MODEL_CARD.md.
- Allal, L. B., Lozhkov, A., Bakouch, E., Blázquez, G. M., Penedo, G., Tunstall, L., Marafioti, A., Kydlíček, H., Lajarín, A. P., Srivastav, V., Lochner, J., Fahlgren, C., Nguyen, X.-S., Fourrier, C., Burtenshaw, B., Larcher, H., Zhao, H., Zakka, C., Morlon, M., Raffel, C., von Werra, L., and Wolf, T. Smollm2: When smol goes big – data-centric training of a small language model, 2025. URL <https://arxiv.org/abs/2502.02737>.
- Biderman, S., Schoelkopf, H., Anthony, Q. G., Bradley, H., O’Brien, K., Hallahan, E., Khan, M. A., Purohit, S., Prashanth, U. S., Raff, E., et al. Pythia: A suite for analyzing large language models across training and scaling. In *International Conference on Machine Learning*, pp. 2397–2430. PMLR, 2023.
- Bloom, S., Brumberg, J., Fisk, I., Harrison, R., Hull, R., Ramasubramanian, M., Van Vliet, K., and Wing, J. Empire ai: A new model for provisioning ai and hpc for academic research in the public good. In *Practice and Experience in Advanced Research Computing 2025: The Power of Collaboration*, PEARC ’25, New York, NY, USA, 2025. Association for Computing Machinery. ISBN 9798400713989. doi: 10.1145/3708035.3736070. URL <https://doi.org/10.1145/3708035.3736070>.
- Chang, H.-S. and McCallum, A. Softmax bottleneck makes language models unable to represent multi-mode word distributions. In Muresan, S., Nakov, P., and Villavicencio, A. (eds.), *Proceedings of the 60th Annual Meeting of the Association for Computational Linguistics (Volume 1: Long Papers)*, pp. 8048–8073, Dublin, Ireland, May 2022. Association for Computational Linguistics. doi: 10.18653/v1/2022.acl-long.554. URL <https://aclanthology.org/2022.acl-long.554>.
- Finlayson, M., Hewitt, J., Koller, A., Swayamdipta, S., and Sabharwal, A. Closing the curious case of neural text degeneration. In *The Twelfth International Conference on Learning Representations*, 2024. URL <https://openreview.net/forum?id=dONpC9GL1o>.
- Ganea, O., Gelly, S., Becigneul, G., and Severyn, A. Breaking the softmax bottleneck via learnable monotonic pointwise non-linearities. In Chaudhuri, K. and Salakhutdinov, R. (eds.), *Proceedings of the 36th International Conference on Machine Learning*, volume 97 of *Proceedings of Machine Learning Research*, pp. 2073–2082. PMLR, 09–15 Jun 2019. URL <https://proceedings.mlr.press/v97/ganea19a.html>.
- Gao, J., He, D., Tan, X., Qin, T., Wang, L., and Liu, T. Representation degeneration problem in training natural language generation models. In *International Conference on Learning Representations*, 2019. URL <https://openreview.net/forum?id=SkEYoJRqtm>.
- Gao, L., Biderman, S., Black, S., Golding, L., Hoppe, T., Foster, C., Phang, J., He, H., Thite, A., Nabeshima, N., Presser, S., and Leahy, C. The pile: An 800gb dataset of diverse text for language modeling, 2020.
- Godey, N., de la Clergerie, É. V., and Sagot, B. Why do small language models underperform? studying language model saturation via the softmax bottleneck. In *First*

- Conference on Language Modeling*, 2024. URL <https://openreview.net/forum?id=MoitXWlXcS>.
- Grivas, A., Bogoychev, N., and Lopez, A. Low-rank softmax can have unargmaxable classes in theory but rarely in practice. In Muresan, S., Nakov, P., and Villavicencio, A. (eds.), *Proceedings of the 60th Annual Meeting of the Association for Computational Linguistics (Volume 1: Long Papers)*, pp. 6738–6758, Dublin, Ireland, May 2022. Association for Computational Linguistics. doi: 10.18653/v1/2022.acl-long.465. URL <https://aclanthology.org/2022.acl-long.465/>.
- Gu, A. and Dao, T. Mamba: Linear-time sequence modeling with selective state spaces. In *First Conference on Language Modeling*, 2024. URL <https://openreview.net/forum?id=tEYskw1VY2>.
- Hoffmann, J., Borgeaud, S., Mensch, A., Buchatskaya, E., Cai, T., Rutherford, E., de Las Casas, D., Hendricks, L. A., Welbl, J., Clark, A., Hennigan, T., Noland, E., Millican, K., van den Driessche, G., Damoc, B., Guy, A., Osindero, S., Simonyan, K., Elsen, E., Rae, J. W., Vinyals, O., and Sifre, L. Training compute-optimal large language models, 2022.
- Hu, S., Tu, Y., Han, X., Cui, G., He, C., Zhao, W., Long, X., Zheng, Z., Fang, Y., Huang, Y., Zhang, X., Thai, Z. L., Wang, C., Yao, Y., Zhao, C., Zhou, J., Cai, J., Zhai, Z., Ding, N., Jia, C., Zeng, G., dahai li, Liu, Z., and Sun, M. MiniCPM: Unveiling the potential of small language models with scalable training strategies. In *First Conference on Language Modeling*, 2024. URL <https://openreview.net/forum?id=3X2L2TfR0f>.
- Kanai, S., Fujiwara, Y., Yamanaka, Y., and Adachi, S. Sigsoftmax: Reanalysis of the softmax bottleneck. In Bengio, S., Wallach, H., Larochelle, H., Grauman, K., Cesa-Bianchi, N., and Garnett, R. (eds.), *Advances in Neural Information Processing Systems*, volume 31. Curran Associates, Inc., 2018. URL https://proceedings.neurips.cc/paper_files/paper/2018/file/9dcb88e0137649590b755372b040afad-Paper.pdf.
- Kaplan, J., McCandlish, S., Henighan, T., Brown, T. B., Chess, B., Child, R., Gray, S., Radford, A., Wu, J., and Amodei, D. Scaling laws for neural language models. *ArXiv*, abs/2001.08361, 2020. URL <https://api.semanticscholar.org/CorpusID:210861095>.
- Mircea, A., Lobacheva, E., and Rish, I. Gradient descent in language model training and saturation. In *High-dimensional Learning Dynamics 2024: The Emergence of Structure and Reasoning*, 2024. URL <https://openreview.net/forum?id=tJj3psv9nm>.
- Penedo, G., Kydlíček, H., allal, L. B., Lozhkov, A., Mitchell, M., Raffel, C., Werra, L. V., and Wolf, T. The fineweb datasets: Decanting the web for the finest text data at scale. In *The Thirty-eight Conference on Neural Information Processing Systems Datasets and Benchmarks Track*, 2024. URL <https://openreview.net/forum?id=n6SCKn2QaG>.
- Petty, J., Steenkiste, S., Dasgupta, I., Sha, F., Garrette, D., and Linzen, T. The impact of depth on compositional generalization in transformer language models. In Duh, K., Gomez, H., and Bethard, S. (eds.), *Proceedings of the 2024 Conference of the North American Chapter of the Association for Computational Linguistics: Human Language Technologies (Volume 1: Long Papers)*, pp. 7239–7252, Mexico City, Mexico, June 2024. Association for Computational Linguistics. doi: 10.18653/v1/2024.naacl-long.402. URL <https://aclanthology.org/2024.naacl-long.402/>.
- Radford, A., Wu, J., Child, R., Luan, D., Amodei, D., and Sutskever, I. Language models are unsupervised multitask learners. 2019.
- Team, Q. Qwen3 technical report, 2025. URL <https://arxiv.org/abs/2505.09388>.
- Yang, S., Kautz, J., and Hatamizadeh, A. Gated delta networks: Improving mamba2 with delta rule. In *The Thirteenth International Conference on Learning Representations*, 2025. URL <https://openreview.net/forum?id=r8H7xhYPwz>.
- Yang, Z., Dai, Z., Salakhutdinov, R., and Cohen, W. W. Breaking the softmax bottleneck: A high-rank RNN language model. In *International Conference on Learning Representations*, 2018. URL <https://openreview.net/forum?id=HkwZSG-CZ>.
- Yang, Z., Luong, T., Salakhutdinov, R. R., and Le, Q. V. Mixtape: Breaking the softmax bottleneck efficiently. In Wallach, H., Larochelle, H., Beygelzimer, A., d’Alché-Buc, F., Fox, E., and Garnett, R. (eds.), *Advances in Neural Information Processing Systems*, volume 32. Curran Associates, Inc., 2019. URL https://proceedings.neurips.cc/paper_files/paper/2019/file/512fc3c5227f637e41437c999a2d3169-Paper.pdf.
- Ye, T., Dong, L., Xia, Y., Sun, Y., Zhu, Y., Huang, G., and Wei, F. Differential transformer. In *The Thirteenth International Conference on Learning Representations*,

2025. URL <https://openreview.net/forum?id=OvoCmlgGhN>.

Yun, C., Bhojanapalli, S., Rawat, A. S., Reddi, S., and Kumar, S. Are transformers universal approximators of sequence-to-sequence functions? In *International Conference on Learning Representations, 2020*. URL <https://openreview.net/forum?id=ByxRM0Ntvr>.

A. Proofs

A.1. Proposition 2.4

Proof. If $D = 2$, we can pick rows of W as distinct points on the unit circle. We then set:

$$H_i = \alpha_i W_{\arg \max(\tilde{N}_i)}$$

with $\alpha_i \geq 0$. We clearly have:

$$\begin{cases} \lim_{\alpha_i \rightarrow 0} \sigma(H_i W^\top)_{i, \arg \max(\tilde{N}_i)} = \frac{1}{V} \\ \lim_{\alpha_i \rightarrow +\infty} \sigma(H_i W^\top)_{i, \arg \max(\tilde{N}_i)} = 1 \end{cases}$$

By definition, $\tilde{N}_{i, \arg \max(\tilde{N}_i)} \in [\frac{1}{V}, 1]$. Hence, by continuity of the softmax function, for all $i \in [1, C]$ and $\varepsilon > 0$, there exists α_i that satisfies Equation (5).

For $D > 2$, we can work on the first two dimensions of H and W and zero-out all other entries to reach the same conclusion. \square

A.2. Proposition 2.5

Proof. We introduce P^u and \tilde{N}^u , where we extract rows that correspond to \mathcal{C}^u from P and \tilde{N} . As $P_{ij} \in]0, 1[$, we have:

$$(P^u - \tilde{N}^u)_{ij} \begin{cases} < 0 \text{ if } j = w_{s,t} \\ > 0 \text{ else.} \end{cases}$$

We also note that

$$\sum_j (P^u - \tilde{N}^u)_{ij} = \sum_j (P - \tilde{N})_{ij} = 1 - 1 = 0$$

Let us now have P^{uu} and \tilde{N}^{uu} by extracting columns from P^u and \tilde{N}^u that correspond to \mathcal{C}^{uu} . We thus notice that \tilde{N}^{uu} corresponds to the identity $I_{|\mathcal{C}^{uu}|}$ up to a permutation of rows. We thus rearrange the rows of P^{uu} and \tilde{N}^{uu} so that $\tilde{N}^{uu} = I_{|\mathcal{C}^{uu}|}$ without loss of generality. This implies that

$$(P^{uu} - \tilde{N}^{uu})_{ij} \begin{cases} < 0 \text{ if } i = j \\ > 0 \text{ else.} \end{cases}$$

As we only removed columns where coefficients of $(P^u - \tilde{N}^u)$ were positive, we also have

$$\sum_j (P^{uu} - \tilde{N}^{uu})_{ij} \begin{cases} < 0 \text{ if } |\mathcal{C}^{uu}| < V \\ = 0 \text{ if } |\mathcal{C}^{uu}| = V \end{cases}$$

If $|\mathcal{C}^{uu}| = V$, then $(P^{uu} - \tilde{N}^{uu})$ is analogous to the Laplacian of a fully connected graph with V vertices, and has rank $V - 1$. Else, then $(P^{uu} - \tilde{N}^{uu})$ is strictly diagonally

dominant, and is full-rank by Gershgorin's circle theorem. As $(P^{uu} - \tilde{N}^{uu})$ is a submatrix of $(P - \tilde{N})$, we have

$$\text{rank}(P - \tilde{N}) \geq \text{rank}(P^{uu} - \tilde{N}^{uu}) = \min(|\mathcal{C}^{uu}|, V - 1)$$

\square

A.3. Proposition 2.7

Proof. By the definition of \mathcal{C}_B^u , each context has a unique and distinct next token in batch \mathcal{B} while having multiple possible next tokens in dataset X . Under condition (8) with sufficiently small ε_B , the submatrix of $(P_\theta - \tilde{N}^B)$ corresponding to rows \mathcal{C}_B^u preserves the sign pattern of $(\tilde{N} - \tilde{N}^B)$ on these rows.

Following the construction in Proposition 2.5, we extract rows from \mathcal{C}_B^u and columns corresponding to the distinct unique batch tokens. Since these tokens are distinct by assumption, we obtain a square submatrix of size $|\mathcal{C}_B^u| \times |\mathcal{C}_B^u|$.

If $|\mathcal{C}_B^u| = V$, the connectivity assumption ensures this submatrix is analogous to the Laplacian of a connected graph, yielding rank $V - 1$.

If $|\mathcal{C}_B^u| < V$, the same argument as in the proof of Proposition 2.5 establishes strict diagonal dominance, hence full rank $|\mathcal{C}_B^u|$ by Gershgorin's circle theorem.

Therefore $\text{rank}(P_\theta - \tilde{N}^B) \geq \min(|\mathcal{C}_B^u|, V - 1)$. \square

B. Convention for log

The element-wise log function is not defined for null entries, which can be expected to be observed often in N and \tilde{N} matrices. To avoid complex notations, we take advantage of the limit of $x \rightarrow x \log x$ in 0^+ and we define

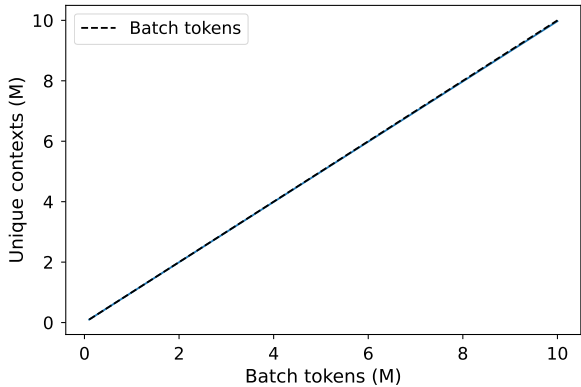
$$\langle X, \log X \rangle_F := \sum_{ij} \mathbf{1}_{X_{ij}} X_{ij} \log X_{ij}$$

C. Empirical Justifications for Assumptions

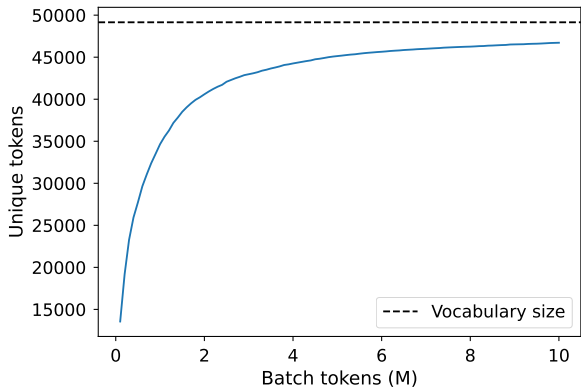
This section reports basic experiments that help justify the assumptions made in Proposition 2.5 and Proposition 2.7 for natural language data.

In Figure 9, we compute basic statistics about unique tokens and contexts in batches of Fineweb documents. The results indicate that nearly all observed contexts are unique, and that most tokens appear at least once for batches of usual sizes (up to a few million tokens). This suggests that the bound in Proposition 2.5 should take high values, as unique contexts made of tokens spanning most of the vocabulary leads to bigger \mathcal{C}^{uu} sets.

In Figure 10, we measure the next-token entropy distribution for Llama-3.1-8B on Fineweb, as a proxy of \tilde{N} . These



(a) Unique contexts count



(b) Unique tokens count

Figure 9. Unique tokens/contexts count as batch size increases. We use the SmolLM2 tokenizer on Fineweb documents.

results indicate that this distribution has relatively scattered support, with a non-negligible number of contexts resulting in entropy levels > 5 . Following the connection made in Proposition 2.7 between \tilde{N} and adjacency matrices, these contexts are likely to act as highly connected vertices, boosting the connectivity of the underlying graph.

D. Cosine-Similarity Analysis of the Null-Space Projection

In Figure 11, we report the average cosine similarity between the logit gradient and its projection on the complement of $\ker(W_\theta^\top)$, which can be framed as the part of the gradient that is visible for all preceding parameters. We observe that most values are comprised between 0.1 and 0.3 showing that the projection is in general mildly aligned with the original gradient. This completes Figure 6 that only considers gradient norm.

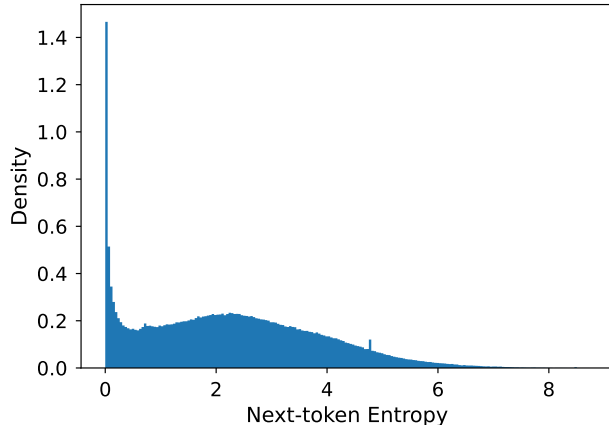


Figure 10. Next-token entropy distribution for Llama-3.1-8B on Fineweb documents.

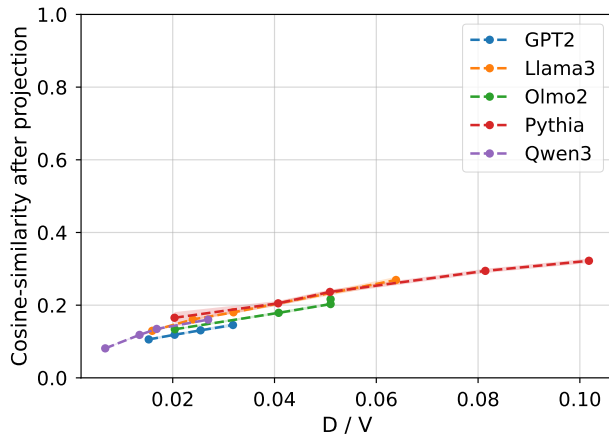


Figure 11. Average cosine-similarity between projected and original gradient as a function of D/V , for several model families.

E. Analysis of the Gradient Compression

In Figure 12, we report additional results for the experiment led in Section 3.3 for Llama-3.1-8B and OLMo2-32B. We reach similar conclusions as for Llama-3.1-70B, namely that the main components of the gradients are smoothed by compression, and the tail of coefficients is noisier after projection.

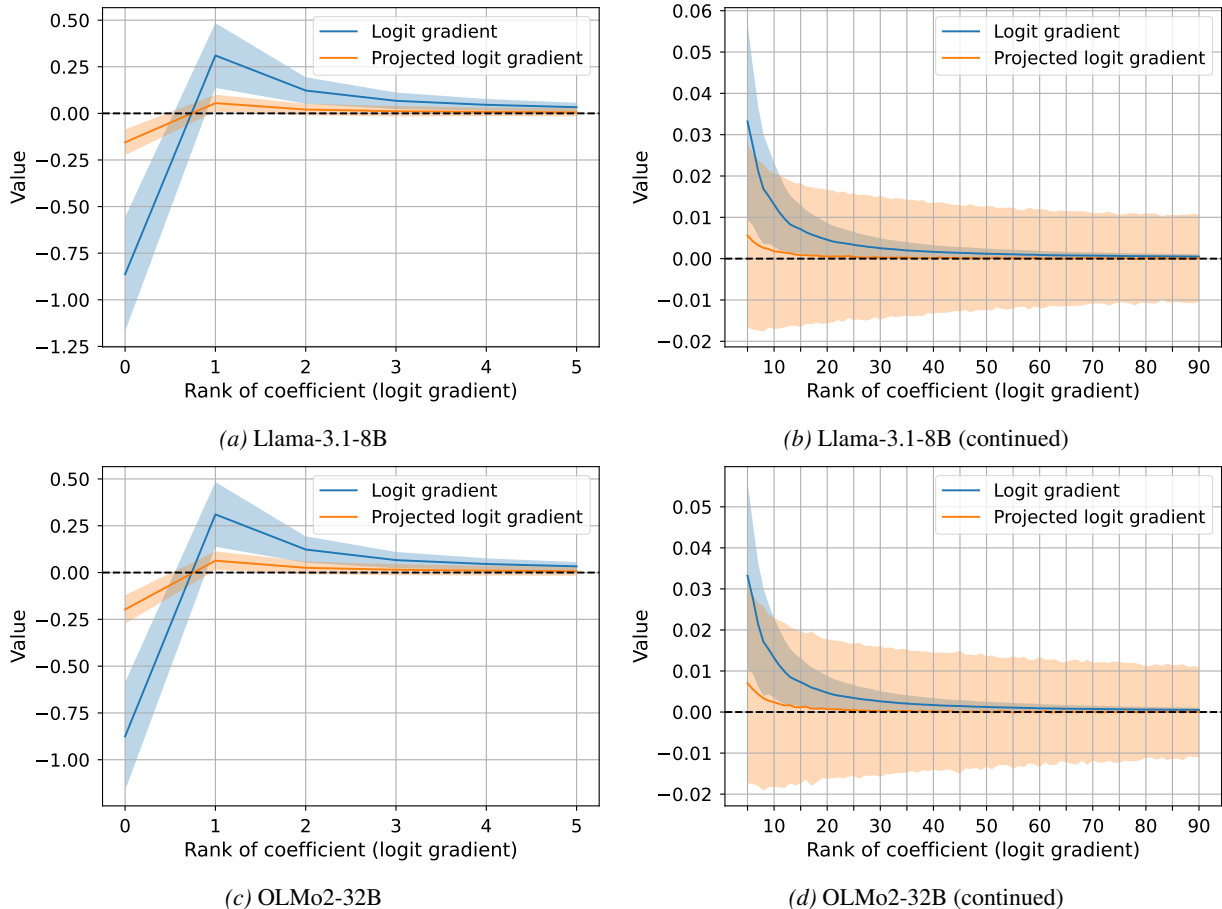


Figure 12. Average full and projected logits gradient coefficients, sorted by absolute values of the full gradient. The gradients are taken for Llama-3.1-8B and OLMo2-32B on Fineweb documents. The plots on the left-hand side focuses on the main coefficients, while the plots on the right-hand side zooms in on smaller coefficients. The standard deviation is reported using filled areas around the curves.

F. Downstream evaluation – Detailed results

In Table 2, we provide a detailed report of zero-shot performance of our rank-constrained models along training. We observe that, despite some benchmarks being more prone to variance effects, the overall trend favors models with higher values of D . We also report a graphical visualization in Figure 13 to facilitate analysis.

G. Experimental setups

G.1. SpamLang Experiments

We report hyperparameters for SpamLang experiments in Table 3. Additionally, our initial experimentations on the impact of weight decay on the training dynamics showed minimal impact. We ran experiments for $D = 32, 768$ using a learning rate of $1e-4$, and obtain final losses within the $[0.2, 0.4]$ range.

Additionally, we provide a side-by-side comparison of our learning rate and vocabulary size sweeps in Figure 14.

G.2. Pretraining Experiments

We report hyperparameters for our pretraining experiments in Table 4. We perform the decay phase of the WSD schedule at 3 intermediate steps:

- After 80,000 operations, where we decay for 5000 steps;
- After 120,000 operations, where we decay for 10000 steps;
- After 170,000 operations, where we decay for 10000 steps.

We adjust the decay length to remain within a 5-10% ratio of the total training steps. For every model, the decay phase is performed on the same data as the stable phase. We observe considerable performance gains during the decay phase, as reported in Hu et al. (2024).

The LM Head is a Gradient Bottleneck

D	ARC-C	ARC-E	HellaSwag	PIQA	SciQ	OpenBookQA	Lambada ↓	Avg.	Avg. (weighted)
5B tokens									
32	23.63	42.21	33.17	60.88	50.40	30.20	593.70	40.08	39.22
64	25.77	45.50	34.57	62.62	60.50	31.80	186.90	43.46	41.46
128	26.96	51.30	36.31	64.36	66.60	34.00	104.50	46.59	43.96
256	28.24	52.23	37.39	64.58	69.30	33.40	70.99	47.52	44.93
512	27.82	53.41	37.66	62.68	72.90	32.40	62.47	47.81	45.06
1024	28.84	52.02	38.65	66.05	72.40	31.80	56.16	48.29	46.01
2048	28.84	55.09	38.64	66.16	73.70	31.60	55.75	49.01	46.50
4096	29.10	53.79	38.87	66.54	72.40	32.60	54.39	48.88	46.49
8.5B tokens									
32	26.11	43.43	34.99	60.72	53.20	32.20	496.49	41.77	40.74
64	27.22	47.52	36.90	64.47	61.80	31.20	162.42	44.85	43.48
128	26.54	52.06	37.63	64.74	67.50	35.80	85.05	47.38	44.92
256	27.90	54.80	38.80	66.21	73.10	32.80	59.74	48.94	46.49
512	27.73	52.95	39.65	66.21	72.90	34.60	52.77	49.01	46.75
1024	28.41	55.39	40.90	66.32	73.40	32.40	45.46	49.47	47.79
2048	31.40	55.85	41.09	66.87	74.10	33.60	45.50	50.48	48.31
4096	29.69	56.10	41.78	67.36	72.40	35.80	45.23	50.52	48.67
11B tokens									
32	25.94	44.19	35.70	61.86	52.90	31.60	406.56	42.03	41.37
64	28.58	47.52	37.69	64.09	61.00	32.20	129.72	45.18	43.92
128	26.28	50.38	38.48	64.85	64.40	33.20	73.17	46.27	44.93
256	28.75	54.92	39.81	67.03	71.70	32.20	47.94	49.07	47.17
512	30.29	54.59	40.99	66.59	69.70	33.20	43.29	49.23	47.72
1024	29.86	55.77	41.41	67.79	73.80	33.60	38.06	50.37	48.52
2048	30.20	55.18	42.11	67.79	73.80	34.00	37.58	50.51	48.86
4096	31.06	56.52	42.64	68.72	71.30	34.40	37.27	50.77	49.41

Table 2. Benchmark scores grouped by training tokens (5B, 8.5B, 11B) and ordered by effective hidden dimension D . We report both weighted and unweighted averages.

The LM Head is a Gradient Bottleneck

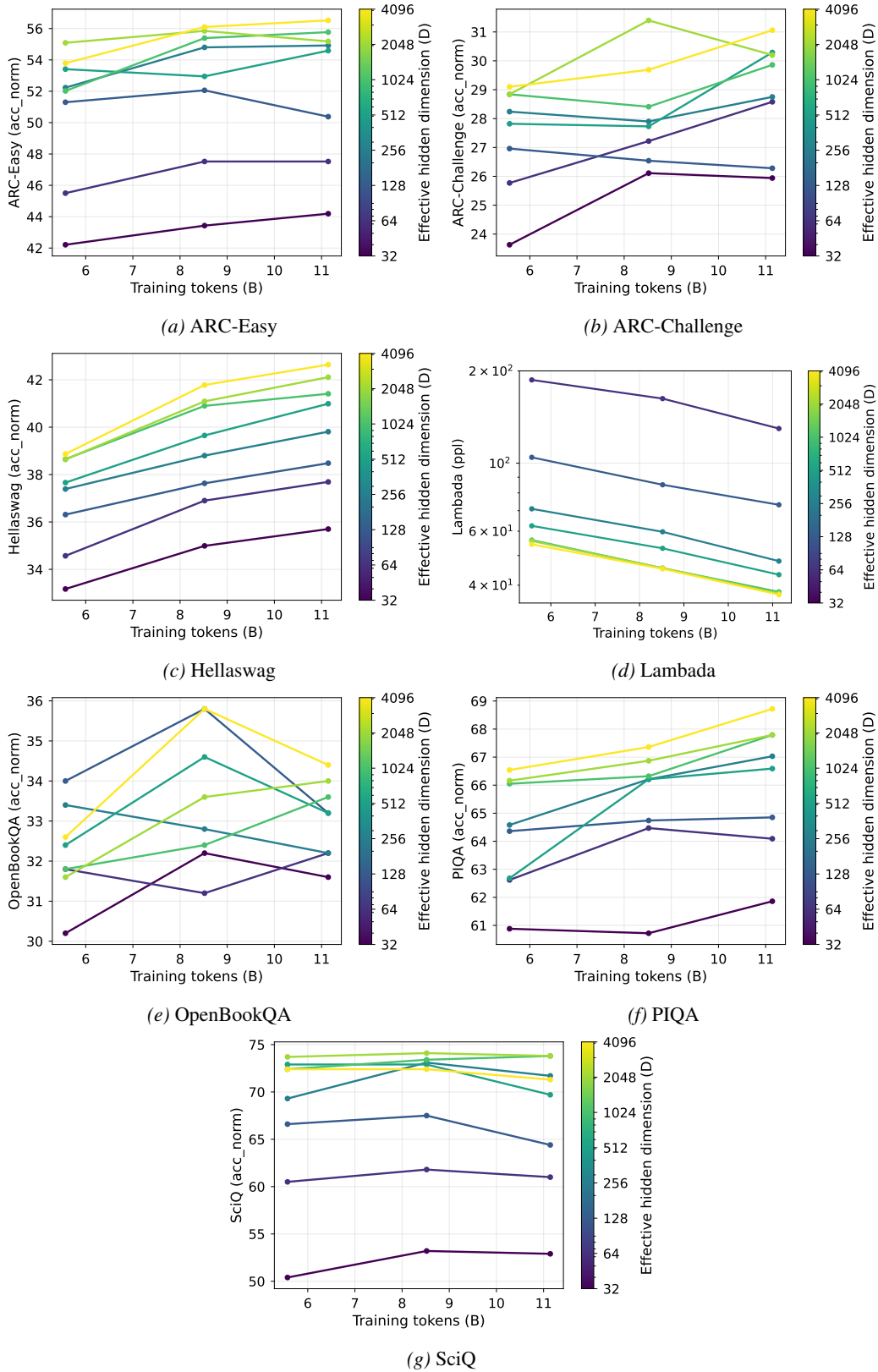


Figure 13. Downstream scores evolution along training for different benchmarks.

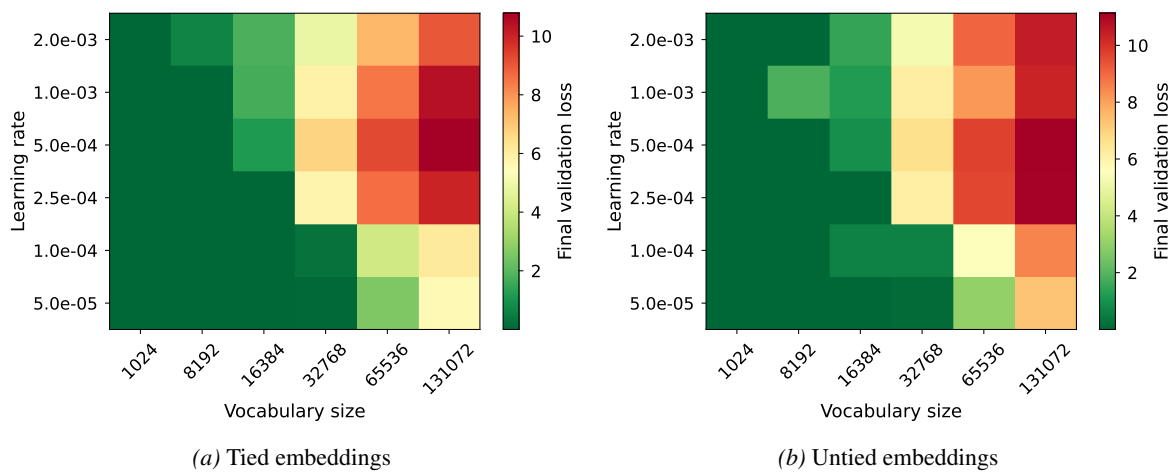


Figure 14. Final validation loss for 106M (non-embedding) parameter Transformer models trained on the `SpamLang` synthetic language for various vocabulary sizes and learning rates. We report untied and tied embedding setups, and observe no strong effect from this hyper-parameter choice. The hidden dimension is set to 576 for all models.

Hyperparameter	Value
Num. Layers	30
Head Dimension	64
Num. Attention Heads	9
Num. KV Heads	3
Hidden size	576
Intermediate size	1536
Precision	Mixed (bfloat16)
Sequence Length	64
Batch Size	128
Total Training Steps	5000
Warmup Steps	500
Weight Decay	0.01
Optimizer	AdamW
Adam β_1, β_2	(0.9, 0.95)
Adam ϵ	1×10^{-8}
Learning Rate Schedule	Cosine Decay
Gradient Clipping	1.0

Table 3. Training hyperparameters used for the SpamLang experiment. Experiments were run on single A6000 NVIDIA GPUs.

Hyperparameter	Value
Num. Layers	6
Head Dimension	128
Num. Attention Heads	32
Hidden size	4096
Intermediate size	16,384
Weight Tying	No
Precision	Mixed (bfloat16)
Sequence Length	512
Train Batch Size	128
Total Training Steps	170,000
Learning Rate	3×10^{-4}
Warmup Steps	2000
Cooldown Steps	10,000
Weight Decay	0.1
Optimizer	AdamW
Adam β_1, β_2	(0.9, 0.95)
Adam ϵ	1×10^{-8}
LR Schedule	Warm-up Stable Decay (WSD)
Decay Type	Cosine (5-10%)
Gradient Clipping	1.0

Table 4. Training hyperparameters used for the pretraining experiments with constrained heads. Experiments were run on B200 GPUs, totaling ~ 760 hours.